

Evaluation of the particle-based Bhatnagar-Gross-Krook method in hypersonic non-equilibrium flows

Woonghwi Park¹, Eunji Jun²

Abstract

In hypersonic flows, non-equilibrium flow characteristics are present. To accurately understand such flows, it is essential to obtain the velocity distribution function using a stochastic approach. In this study, the accuracy of the particle-based Bhatnagar-Gross-Krook (BGK) method in the analysis of the velocity distribution function is evaluated in comparison to the Direct Simulation Monte Carlo method. In particular, deviations from the Maxwellian distribution are identified in the velocity distribution function under non-equilibrium flow conditions, and differences in how different BGK models represent this are highlighted. As a result, the Shakhov BGK model is found to be more accurate in reproducing the velocity distribution function than the ellipsoidal-statistical BGK model.

Keywords: Direct simulation Monte-Carlo (DSMC), particle-based Bhatnagar-Gross-Krook (BGK) method, velocity distribution function, non-equilibrium flows

1. Introduction

In hypersonic flows, non-equilibrium characteristics may exist where macroscopic properties can change rapidly over the length scale of the mean free path or over the time scale of the mean collision time. Continuum fluid mechanics may not be sufficient to represent such non-equilibrium characteristics. Instead, it is better to focus on the individual motion of each fluid particle. The state of gas particle motion is represented by the velocity distribution function. The velocity distribution function describes the probabilistic distribution of gas particles over the phase space, which comprises physical space and velocity space. The velocity distribution function follows a Maxwellian distribution at equilibrium. However, in non-equilibrium flow, a non-Maxwellian distribution may appear.

The Boltzmann equation governs the velocity distribution function. Numerical methods have been developed to solve the Boltzmann equation because there is no analytical solution. Deterministic approaches involve discretizing the velocity distribution function in phase space [1]. However, these methods can be computationally expensive and require excessive memory usage, especially in hypersonic flows where the velocity range is extensive. Alternatively, stochastic approaches can be employed. These approaches resolve the velocity distribution function in a probabilistic manner. Although the resulting velocity distribution function is subject to statistical errors, stochastic approaches are suitable for interpreting hypersonic flows due to advantages in memory and computational cost compared to deterministic approaches.

The direct simulation Monte-Carlo (DSMC) method is the most widely recognized stochastic approach [2]. The DSMC method interprets the velocity distribution function using computational particles that represent the ensemble of actual particles. Theoretical proof demonstrates that the solutions of the DSMC method are equivalent to those of the Boltzmann equation [3]. Also, the DSMC method has been experimentally verified to accurately interpret velocity distribution functions within shock waves [4]. Recent advancements in DSMC have expanded its application to analyze instabilities, turbulences, and interactions with porous media [5-7].

The particle-based BGK method is a stochastic approach that can be used as an alternative to solve the velocity distribution function [8-11]. This method solves the BGK equation, which approximates the

¹ Graduate student, Department of Aerospace Engineering, Korea Advanced Institute of Science and Technology, Daejeon 34141, South Korea, whpark@kaist.ac.kr

² Assistant professor, Department of Aerospace Engineering, Korea Advanced Institute of Science and Technology, Daejeon 34141, South Korea, eunji.jun@kaist.ac.kr

change in the velocity distribution function due to collisions with a linear relaxation towards local equilibrium [12]. The BGK equation is based on the Boltzmann H-theorem, which states that collisions among molecules contribute to the increase in the gas's entropy. The BGK equation is most accurate in the continuum limit, where it converges to the Navier-Stokes equation. Therefore, the particle-based BGK method is only reliable for flows near equilibrium. The particle-based Fokker-Planck method is another significant stochastic method [13-19]. This method interprets changes in the velocity distribution function resulting from collisions as a combination of particle drift motion and random motion.

It is important to evaluate the accuracy of the particle-based BGK method in non-equilibrium flows, as its accuracy is only guaranteed close to equilibrium. This evaluation generally involves comparing the flow analysis results obtained from the BGK method with those obtained from the DSMC method. Previous studies have mostly been limited to comparing the flow's macroscopic properties, such as density, velocity, and temperature, which are the moments of the velocity distribution function [9]. Fei et al. compared the third- and fourth-order moments to evaluate the accuracy of different BGK and FP methods [20]. However, in case of non-Maxwellian distributions, the individual moments are insufficient to represent the velocity distribution function. Therefore, it is necessary to focus on the shape of the velocity distribution function itself.

In this study, a direct comparison of the velocity distribution function is conducted to evaluate two different particle-based BGK methods: the ellipsoidal-statistical BGK (ESBGK) and Shakhov BGK (SBGK) methods. Two representative cases of non-equilibrium in hypersonic flows are presented. The first case involves hypersonic Couette flow, which represents the non-equilibrium that can occur between hypersonic flow and a fully-accommodative wall boundary. The second case illustrates the changes in the velocity distribution function within the shock wave, where velocity and temperature undergo rapid variations.

2. Governing equations

2.1. Boltzmann equation

The Boltzmann equation expresses the transport of the velocity distribution function in phase space as follows:

$$\frac{\partial}{\partial t}(nf) + v \cdot \frac{\partial}{\partial x}(nf) = \left[\frac{\partial}{\partial t}(nf) \right]_{coll} \quad (1)$$

where n is the number density and $f(x, v, t)$ represents the velocity distribution function. The left-hand side represents the transport due to the translational motion of individual particles in physical space. The Boltzmann collision operator on the right-hand side accounts for the transport in velocity space due to intermolecular collisions as follows:

$$\left[\frac{\partial}{\partial t}(nf) \right]_{coll} = \int_{-\infty}^{\infty} \int_0^{4\pi} n^2 (f^* f_1^* - f f_1) c_r \sigma d\Omega dv \quad (2)$$

where c_r is the relative velocity, σ is the collision cross section, and f, f_1, f^*, f_1^* are the velocity distribution functions of colliding particle pairs. The Boltzmann collision operator assumes that collisions involve only binary interactions between gas molecules, and there is no correlation in the velocities of colliding particle pairs before and after collisions. The integro-differential form of the Boltzmann equation presents challenges for both analytical and numerical solutions due to the complexity introduced by the collision operator.

2.2. BGK equation

To simplify the Boltzmann equation, Bhatnagar et al. proposed the BGK equation, incorporating collision-induced relaxation, as follows:

$$\frac{\partial}{\partial t}(nf) + v \cdot \frac{\partial}{\partial x}(nf) = \left[\frac{\partial}{\partial t}(nf) \right]_{BGK} \quad (3)$$

$$\left[\frac{\partial}{\partial t}(nf) \right]_{BGK} = nv(f_t - f) \quad (4)$$

where ν is the relaxation frequency and f_t is the target distribution [12]. The BGK equation replaces the Boltzmann collision operator with a linear relaxation towards a target distribution. The standard BGK model sets the target distribution as the local Maxwellian distribution, defined as:

$$f_0(v) = \left(\frac{m}{2\pi k_B T} \right)^{\frac{3}{2}} \exp \left[\frac{-mc^2}{2k_B T} \right] \quad (5)$$

where $c = v - u$ is the thermal velocity, $k_B = 1.38 \times 10^{-23} \text{J/K}$ is the Boltzmann constant, T is the temperature, u is the flow velocity, and m is the mass of the particle. The standard BGK model couples the viscosity coefficient and thermal conductivity coefficient in the continuum limit, leading to an incorrect Prandtl number. The viscosity coefficient μ and thermal conductivity coefficient K in the standard BGK model are derived as follows:

$$\mu = \frac{nk_B T}{\nu}, \quad K = C_p \frac{nk_B T}{\nu} \quad (6)$$

where $C_p = 5k_B/2m$ is the specific heat at constant pressure. The Prandtl number is fixed at 1, whereas it should be $2/3$ for a monatomic gas.

The ESBGK and SBGK models were introduced to address this Prandtl number issue [21, 22]. These models maintain a constant relaxation frequency but modify the target distribution function to correct the Prandtl number. The ESBGK model uses an anisotropic Gaussian distribution as the target distribution:

$$f_{ES}(v) = \frac{1}{\sqrt{\det A}} \left(\frac{m}{2\pi k_B T} \right)^{\frac{3}{2}} \exp \left[-\frac{mc^T A^{-1} c}{2k_B T} \right] \quad (7)$$

with the anisotropic matrix

$$A = I - \frac{1 - Pr}{Pr} \left(\frac{3P}{\text{Trace}(P)} - I \right) \quad (8)$$

where I is the identity matrix and $P = \int c \cdot c^T f dv$ is the pressure tensor.

The SBGK equation applies an asymmetric distribution as the target distribution:

$$f_S(v) = f_0 \left[1 + (1 - Pr) \frac{m^2 c \cdot q}{5nk_B^2 T^2} \left(\frac{mc^2}{2k_B T} - \frac{5}{2} \right) \right] \quad (9)$$

with the heat flux vector is defined as:

$$q = \int c c^2 f dv \quad (10)$$

Both the ESBGK and SBGK models correctly interpret the Prandtl number in the continuum limit. However, due to their use of different target distribution functions, there may be differences in how they model the velocity distribution function when deviating from the Maxwellian distribution. It is important to note that the Boltzmann H-theorem is only proven for the ESBGK model. The SBGK equation satisfies the Boltzmann H-theorem only for velocity distribution functions with small perturbation, as it fails to guarantee the positivity of the velocity distribution function.

3. Numerical methods

3.1. DSMC

The DSMC method is used to simulate the velocity distribution function by the stochastic movement of computational particles. By using a sufficient number of computational particles, it is possible to approximate the probability of a particle appearing at a given position and velocity as the probability of a particle at that position and velocity in the velocity distribution function.

The stochastic motion of computational particles adheres to the Boltzmann equation, which includes translational motion and intermolecular collisions. During a discrete time step, each computational particle undergoes constant velocity motion, updating its position without modifying its velocity. The No-Time-Counter (NTC) algorithm is used for intermolecular collisions. The NTC algorithm selects pairs of particles within each computational grid at random and determines the probability of collision based

on the relative velocity of the two particles using an acceptance-rejection method. If the collision is accepted, the particles undergo velocity updates without changing their positions. Post-collision velocities assume elastic collision, and the scattering angle is randomly assigned based on the collision model.

After enough iterations to achieve flow convergence, additional iterations are carried out to sample the positions and velocities of a significant number of computational particles. The sampled data is then used to estimate the velocity distribution function, and desired physical quantities can be obtained by calculating moments of the velocity distribution function for each grid. For example, the velocity is calculated as the average of the velocity distribution function, while the temperature is proportional to the variance of the distribution function. This study uses the SPARTA code, an open-source DSMC code optimized for parallel computing resources [23].

3.2. Particle-based BGK method

The particle-based BGK method simulates a relaxation process instead of intermolecular collisions. During the relaxation process, particles are stochastically selected at each time step to participate in relaxation, and their velocities are reassigned to sampled velocities from the target distribution function. The probability of a particle participating in relaxation is calculated as follows:

$$p = 1 - \exp(-\nu dt) \quad (11)$$

The relaxation frequency can be determined from the local viscosity coefficient. The local viscosity coefficient is dependent on the local temperature as follows:

$$\mu = \mu_{ref} \left(\frac{T}{T_{ref}} \right)^\omega \quad (12)$$

where ω is the viscosity-temperature exponent and μ_{ref}, T_{ref} are the reference viscosity coefficient and temperature, respectively.

To sample velocities from the target distribution function, a random normal vector with zero mean and unit variance in each directions is selected. The random normal vector multiplied by the local thermal velocity yields the velocity sample following the local Maxwellian distribution. To sample the target distribution in the ESBGK equation, velocity sample is multiplied by the square root of the anisotropic matrix A . In the case of the SBGK equation, the acceptance-rejection method is employed. Velocity sample is selected based on the ratio between the probability of having the velocity in the local Maxwellian distribution and in the SBGK target distribution.

The DSMC method guarantees precise conservation of momentum and energy during each collision, whereas the BGK method stochastically conserves momentum and energy before and after relaxation. As the number of iterations increases, fluctuations in total momentum and energy follow a random walk pattern. To address this issue, velocity scaling is applied at each time step to ensure that the momentum and energy of particles within each grid match exactly before and after relaxation.

4. Results

4.1. Couette flow

Couette flow is the flow between two parallel plates at different temperatures and velocities. Both wall boundaries are assumed to be fully accommodative. This means that all particles, after colliding with the wall, follow a Maxwellian distribution with the velocity and temperature of the wall. Because both walls supply momentum to the flow in opposite directions, Couette flow can be considered the simplest form of flow around a surface boundary within hypersonic flow.

In the simulation, the temperatures of the two walls are 273 K and 473K, and their velocities are ± 450 m/s in opposite directions. Three different Knudsen number conditions, 0.01, 0.1 and 1, are applied by varying the flow density. The velocity and temperature distributions within the flow are shown in Fig. 1. In terms of velocity, both the ESBGK and SBGK methods show results consistent with DSMC at Knudsen 0.01 and 0.1. At Knudsen 1, the ESBGK method shows a smaller velocity gradient compared to SBGK. For temperature, at Knudsen 0.01, both BGK methods give accurate results. However, at Knudsen 0.1 and 1, both BGK methods predict a lower maximum temperature.

Nevertheless, the SBGK method is found to predict the temperature near the wall more accurately than ESBGK for all Knudsen numbers.

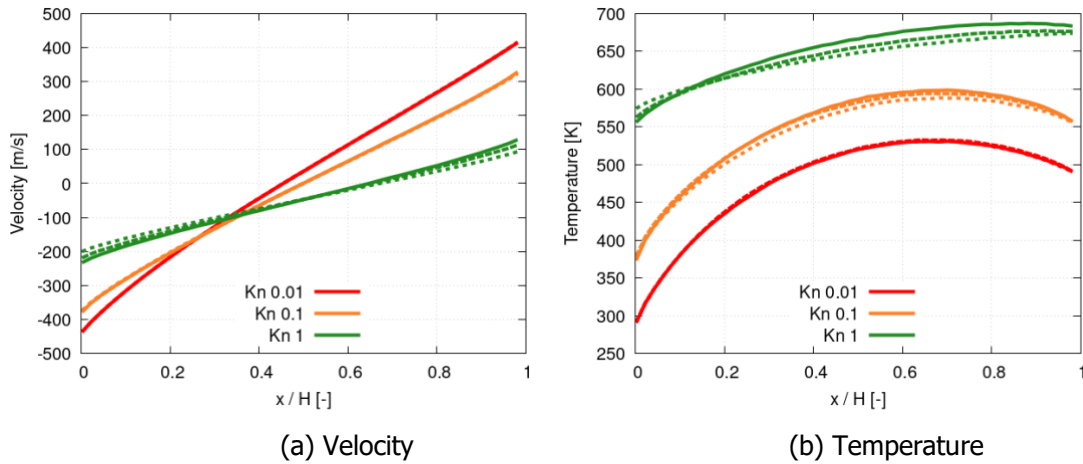
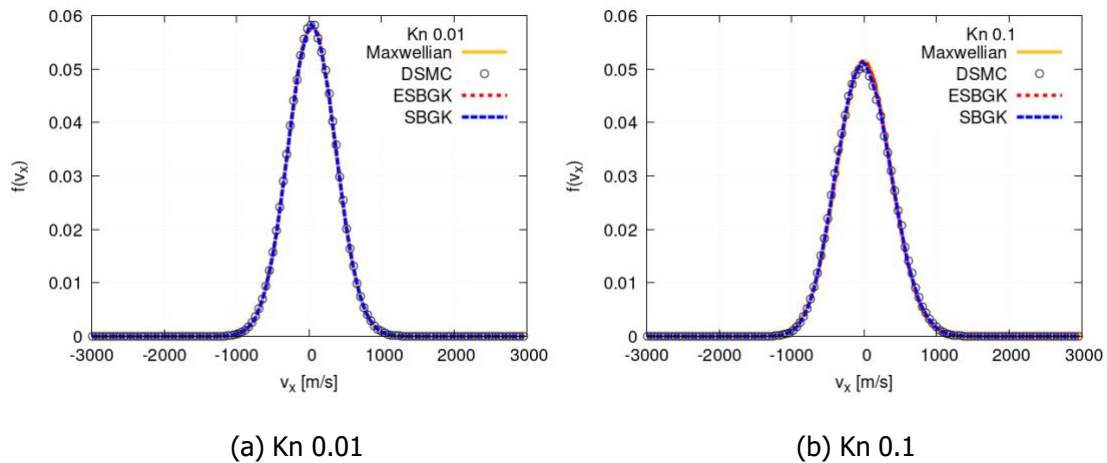
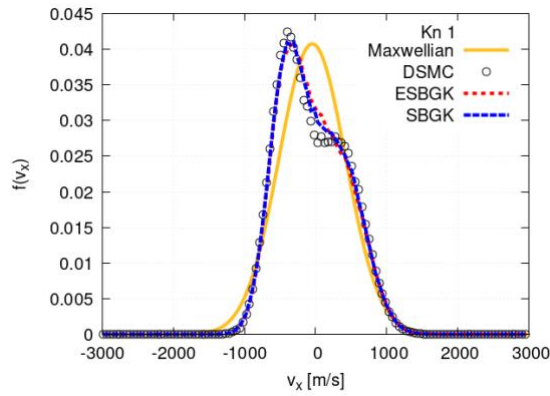


Fig. 1 Velocity and temperature profiles in the Couette flow at different Knudsen numbers. (DSMC results are indicated by solid lines, ESBGK results by dotted lines, and SBGK results by dashed lines)

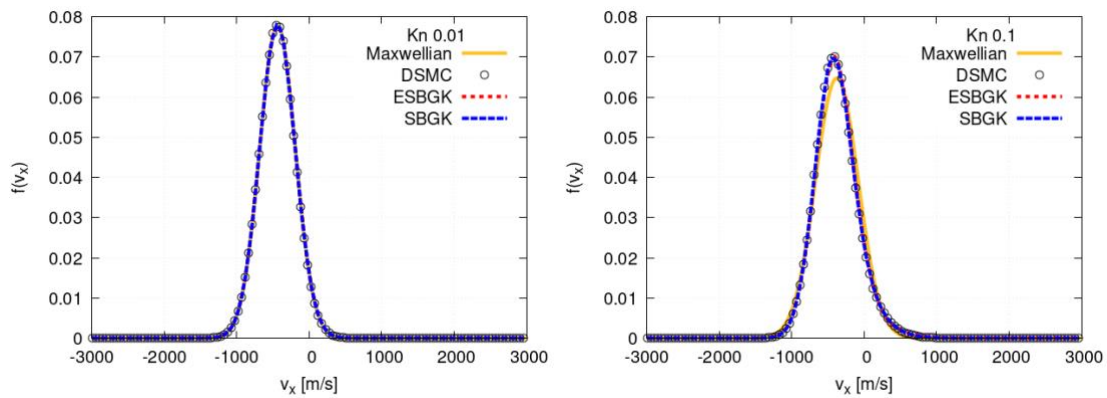
The velocity distribution functions at the center is shown in Figure 2. At Knudsen 0.01, the DSMC results confirm a perfect Maxwellian distribution and both BGK methods give consistent results. At Knudsen 0.1, DSMC shows a lower peak than a Maxwellian distribution at the same temperature. In contrast, both ESBGK and SBGK predict peaks lower than Maxwellian but higher than DSMC. This observation suggests an underestimation of the variance in the velocity distribution function, which contributes to the lower temperature predictions shown in Fig. 1b. At Knudsen 1, the DSMC results deviate significantly from the Maxwellian distribution and show a bimodal shape with two distinct peaks. Similar to the case of Knudsen 0.1, both BGK methods overestimate the particles near the mean velocity, with this feature being more pronounced in the ESBGK method.





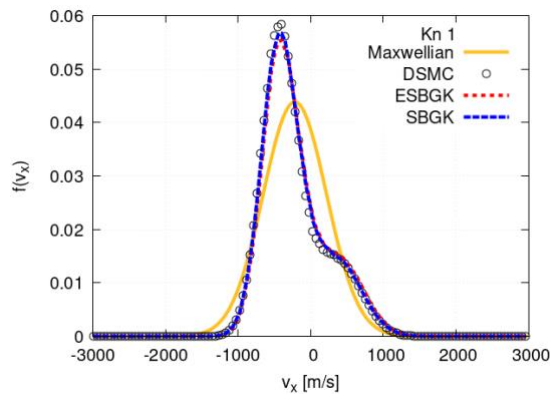
(c) Kn 1

Fig. 2 Velocity distribution functions at the center of Couette flow



(a) Kn 0.01

(b) Kn 0.1



(c) Kn 1

Fig. 3 Velocity distribution functions near the wall of the Couette flow

Next, the velocity distribution function near the wall is shown in Fig. 3. At Knudsen 0.01, the DSMC results agree with the Maxwellian distribution corresponding to the velocity and temperature of the wall, which is also accurately captured by both BGK methods. At Knudsen 0.1, the DSMC results deviate from the local Maxwellian distribution and show a right-skewed shape. Both BGK methods are in good agreement with the DSMC results, accurately predicting the temperature near the wall at Knudsen 0.1, as shown in Fig. 1b. For Knudsen 1, the DSMC results show a right-skewed shape similar to Fig. 2c. Both BGK methods fail to accurately represent the local maximum near the velocity of -450 m/s and

the local minimum near the velocity of 0. In particular, ESBGK shows inaccuracies in predicting the velocity distribution function compared to SBGK.

From the results of the velocity distribution function, it is clear that SBGK is more accurate in predicting the velocity distribution function than ESBGK. The difference between the two BGK models lies in the target distribution function. ESBGK uses an anisotropic Gaussian distribution, which is always symmetrical. This limitation could lead to difficulties in representing asymmetric distributions, such as those near the wall. On the other hand, the target distribution function of SBGK can be asymmetric based on the heat flux, making it relatively more accurate in representing asymmetric distribution functions.

4.2. Normal shock wave

To compare the velocity distribution function within a normal shock wave, the analysis is performed on a Mach 5 steady shock wave. The flow temperature before the shock wave is 300 K and the number density is $1.609 \times 10^{21} \text{ 1/m}^3$. The velocity, temperature and number density after the shock wave are determined according to the Rankine-Hugoniot relation. Note that Park et al. provide a detailed analysis of the normal shock wave [24]. Figure 4 shows the distribution of number density and temperature inside the shock wave. The position where the number density is averaged between upstream and downstream is chosen as the shock center and placed at 0 m. In Fig. 4a, the density increase in the shock wave is observed to occur between -0.02 m and 0.02 m. The results of DSMC and SBGK are in relatively good agreement, but ESBGK tends to overestimate the density near the shock front at -0.01 m, underestimate it between -0.005 m and 0 m around the shock center, and overestimate it between 0.005 m and 0.01 m in the shock rear. The difference between ESBGK and SBGK is also noticeable in the temperature distribution shown in Fig. 4b. The temperature gradient within the shock wave in the SBGK results is in good agreement with the DSMC results. In contrast, ESBGK tends to overestimate the temperature from the shock front at -0.02 m to -0.01 m, underestimate it between -0.005 m and 0 m around the shock center. Note that the temperature increase mostly occurs in the region ahead of the shock center, particularly on the relatively low-density upstream side.

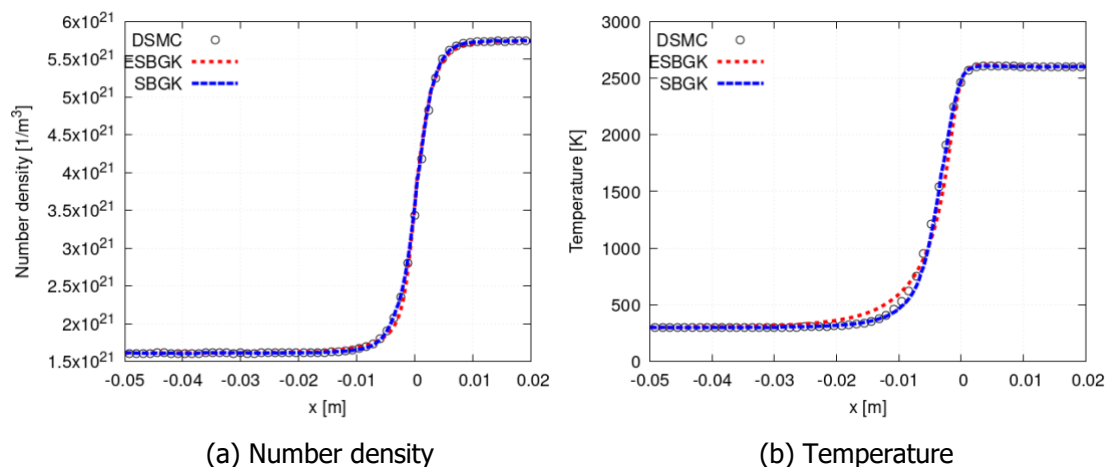


Fig. 4 Number density and temperature profiles in the shock wave

When comparing the velocity distribution function at different positions within the shock wave, it is observed that there is a phase difference between the different methods. This is due to the fact that the velocity distribution function within the shock wave varies with the number density rather than the position. Consequently, comparing the velocity distribution functions at the same position becomes an issue as they correspond to different densities at the same position. To overcome this, comparisons are made at positions with the same normalised density, where n' represents the increase in number density at each position between the upstream and downstream number densities. The position where $n'=50\%$ corresponds to the shock center.

Figure 5 compares the velocity distribution functions at locations where the density is increased by 10%, 20%, 30% and 40% compared to upstream. The velocity distribution functions at the upstream locations where the abrupt increase in flow temperature occurs are compared. It can be seen that the temperature increase is mainly due to the left tail of the velocity distribution function. In Figs. 5a and

5b, SBGK closely matches the DSMC results while ESBGK deviates. Similar to the Couette flow results, this suggests that ESBGK has a weakness in modelling skewed distribution functions. On the other hand, Figs. 5c and 5d show that both BGK methods reproduce the DSMC results relatively accurately.

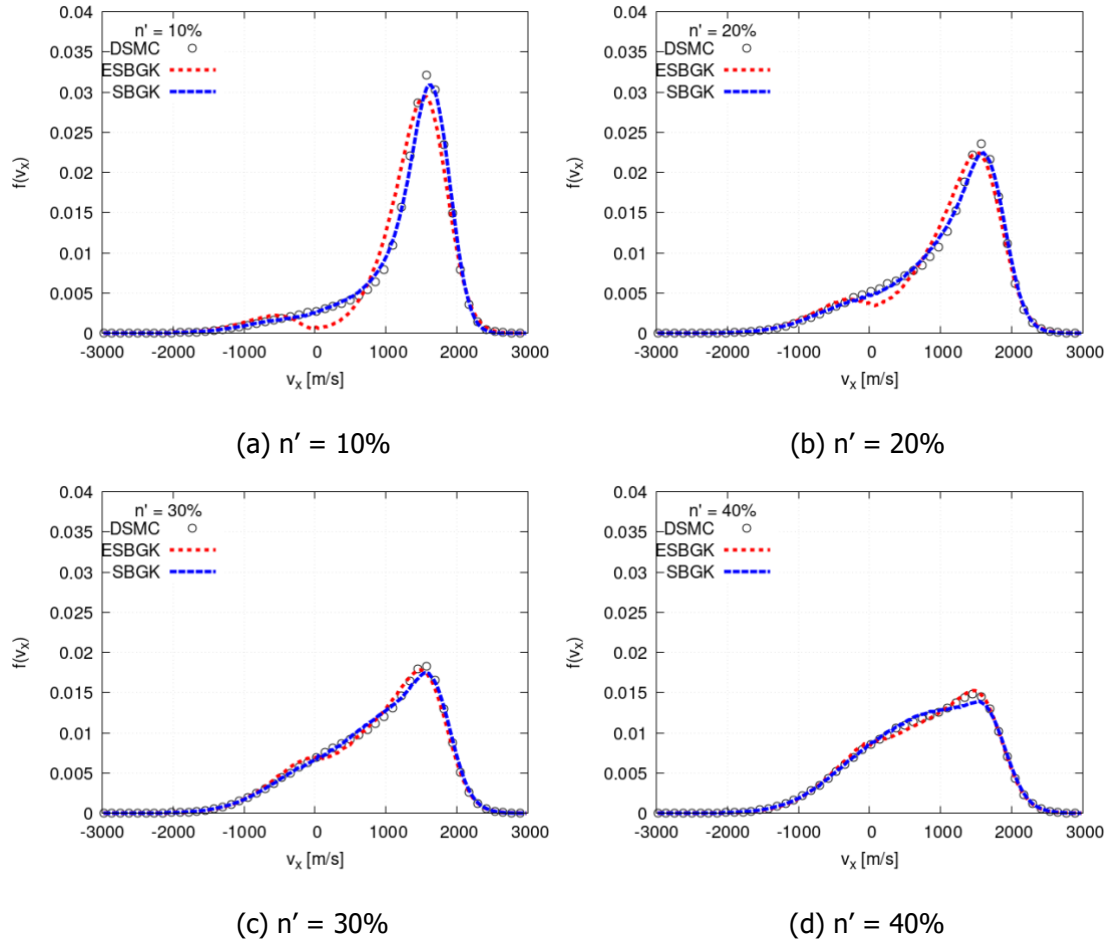


Fig. 5 Velocity distribution functions in the shock wave

5. Conclusion

In this study, hypersonic Couette flow and normal shock wave were analyzed using particle-based flow analysis methods, namely DSMC and the particle-based BGK method. The accuracy of the BGK method was evaluated not only by comparing macroscopic properties such as velocity and temperature but also by observing the similarity of the velocity distribution function. As a result, it was confirmed that the SBGK method is more accurate in simulating the velocity distribution function deviating from the Maxwellian distribution compared to the ESBGK method. In particular, when the velocity distribution function is asymmetric, the ESBGK method shows significant errors, which can be attributed to the fact that the target distribution function of the ESBGK method can only represent symmetric distributions. Therefore, in analyzing the accuracy of stochastic particle methods in non-equilibrium flows such as hypersonic flow, it is essential not only to compare macroscopic properties but also to examine the velocity distribution function to understand the physical significance of each method.

This study focused on the comparison of the steady solutions of the flow, which is suitable for cases where non-Maxwellian distribution functions are caused by the spatial gradient of the flow properties, as in hypersonic flow. However, in cases where the ensemble-averaged velocity distribution function of the flow is Maxwellian but time-averaged fluctuations cause non-equilibrium conditions, the comparison of each analysis method using steady solutions becomes insufficient. Therefore, future studies aim to evaluate the accuracy of unsteady solutions using each BGK method by comparing them with DSMC, thereby providing insight into the accuracy of unsteady flows.

Acknowledgments

This work was supported by Korea Research Institute for defense Technology planning and advancement(KRIT) grant funded by the Korea government(DAPA(Defense Acquisition Program Administration)) (No. KRIT-CT-22-030, Reusable Unmanned Space Vehicle Research Center, 2024)

References

1. Broadwell, J.E.: Study of rarefied shear flow by the discrete velocity method. *J. Fluid Mech.* 19.3, 401-414 (1964)
2. Bird, G.: *Molecular Gas Dynamics and the Direct Simulation of Gas Flows*. Oxford University Press, Oxford (1994)
3. Wagner, W.: A convergence proof for Bird's direct simulation Monte Carlo method for the Boltzmann equation. *J. Stat. Phys.* 66, 1011-1044 (1992)
4. Pham-Van-Diep, G., Erwin D., Muntz E.: Nonequilibrium molecular motion in a hypersonic shock wave. *Science* 245, 624-626 (1989)
5. Gallis, M., et al.: Direct simulation Monte Carlo investigation of the Richtmyer-Meshkov instability. *Phys. Fluids* 27.8 (2015)
6. Gallis, M., et al.: Molecular-level simulations of turbulence and its decay. *Phys. Rev. Lett.* 118.6 (2017)
7. McMullen, R. et al.: Gas-kinetic simulations of compressible turbulence over a mean-free-path-scale porous wall. *AIAA SCITECH 2022 Forum*, 1058 (2022)
8. Gallis, M., Torczynski, J.: The application of the BGK model in particle simulations. 34th Thermophysics Conference (2000)
9. Pfeiffer, M.: Particle-based fluid dynamics: Comparison of different Bhatnagar-Gross-Krook models and the direct simulation Monte Carlo method for hypersonic flows. *Phys. Fluids* 30 (2018)
10. Yao, S., et al.: Extension of the Shakhov Bhatnagar-Gross-Krook model for nonequilibrium gas flows. *Phys. Fluids* 35 (2023)
11. Park, W., Jun, E.: ES-BGK model with internal energy relaxation: Application to hypersonic flow around a cylinder. 34th International Symposium on Shock Waves (2023)
12. Bhatnagar, P.L., Gross, E.P., Krook, M.: A model for collision processes in gases. I. Small amplitude processes in charged and neutral one-component systems. *Phys. Rev.* 94, 511 (1954)
13. Jun, E., et al.: Assessment of the cubic Fokker-Planck-DSMC hybrid method for hypersonic rarefied flows past a cylinder. *Comput. Fluids* 168 (2018)
14. Jun, E., Grabe, M., Hannemann, K.: Cubic Fokker-Planck method for rarefied monatomic gas flow through a slit and an orifice. *Comput. Fluids* 175 (2018)
15. Jun, E., Burt, J., Boyd, I.: All-Particle Multiscale Computation of Hypersonic Rarefied Flow. *AIP Conf.* 1333, 557-562 (2011)
16. Jun, E., Boyd, I., Burt, J.: Assessment of an all-particle hybrid method for hypersonic rarefied flow. 51st AIAA Aerospace Sciences Meeting including the New Horizons Forum and Aerospace Exposition (2013)
17. Kim, S., Jun, E.: A stochastic particle Fokker-Planck method with nonlinear production terms for a variable hard-sphere gas. *Phys. Fluids* 34 (2022)
18. Kim, S., Gorji, H., Jun, E.: Critical assessment of various particle Fokker-Planck models for monatomic rarefied gas flows. *Phys. Fluids* 35 (2023)

19. Kim, S., Jun, E.: A Stochastic Fokker-Planck-Master Model for Diatomic Rarefied Gas Flows. Available at SSRN: <https://ssrn.com/abstract=4562232> or <http://dx.doi.org/10.2139/ssrn.4562232>
20. Fei, F., et al.: A benchmark study of kinetic models for shock waves. *AIAA J.* 58 (2020)
21. Holway, Jr., L.H.: New statistical models for kinetic theory: Methods of construction. *Phys. Fluids* 9, 1658-1673 (1966)
22. Shakhov, E.: Generalization of the Krook kinetic relaxation equation. *Fluid Dyn.* 3, 95-96 (1972)
23. Plimpton, S., et al.: Direct simulation Monte Carlo on petaflop supercomputers and beyond. *Phys. Fluids* 31 (2019)
24. Park, W., et al.: Evaluation of stochastic particle Bhatnagar-Gross-Krook methods with a focus on velocity distribution function. *Phys. Fluids* 36 (2024)